

Magnetic susceptibility and specific heat studies on heavy rare earth ruthenate pyrochlores $R_2Ru_2O_7$ ($R = Gd-Yb$)

Nobuyuki Taira, Makoto Wakeshima and Yukio Hinatsu

Division of Chemistry, Graduate School of Science, Hokkaido University, Kita-ku, Sapporo 060-0810, Japan

Received 19th November 2001, Accepted 14th February 2002

First published as an Advance Article on the web 21st March 2002

Magnetic susceptibility and specific heat measurements were performed for heavy rare earth ruthenate pyrochlores $R_2Ru_2O_7$ ($R = Gd, Tb, Dy, Ho, Er, Tm, \text{ and } Yb$). The compounds of $R = Tb, Er, \text{ and } Yb$ show magnetic transitions at 3.4, 5.4, and 6.3 K, respectively, in the magnetic susceptibility vs. temperature curves. λ -Type anomalies indicating long-range magnetic ordering are observed in the specific heat vs. temperature curves for all of the compounds. At very low temperatures, the presence of short-range magnetic interactions between the rare earth ions for $R = Tb, Er, \text{ and } Yb$ compounds is indicated from both the susceptibility and the specific heat data.

Introduction

In an early work, we reported the results of magnetic susceptibility and magnetic hysteresis measurements on rare earth ruthenate pyrochlores $Y_2Ru_2O_7$ and $Lu_2Ru_2O_7$.¹ Both compounds show magnetic transitions, at 80 and 85 K respectively. Below these temperatures, they transform to a spin-glass state. In these compounds, the magnetic properties should be attributable to the properties of the Ru^{4+} ions in the pyrochlore structure, because both the Y^{3+} ion and the Lu^{3+} ion are diamagnetic.

In the following, we paid attention to the ruthenium pyrochlores $R_2Ru_2O_7$ in which not only the ruthenium ion but also rare earth ions (R^{3+} ions) are paramagnetic, and measured magnetic properties for $R_2Ru_2O_7$ where $R = Pr, Nd, \text{ and } Sm-Yb$.² Among these, $Pr_2Ru_2O_7$, $Nd_2Ru_2O_7$, $Sm_2Ru_2O_7$ and $Eu_2Ru_2O_7$ show magnetic transitions at 165, 150, 135, and 120 K, respectively, and divergence of the ZFC (zero-field-cooled condition) and FC (field-cooled condition) susceptibilities is observed below the magnetic transition temperatures. These results show that below the transition temperatures, the magnetic state of these pyrochlores also transforms to a spin-glass state. No magnetic transition is observed for any of the other studied ruthenium pyrochlores $R_2Ru_2O_7$ ($R = Gd-Yb$) in the temperature range 5–300 K.

For all of the rare earth ruthenate pyrochlores $R_2Ru_2O_7$, a significant λ -type anomaly of the specific heat was found, suggesting that the transition is second-order.^{3–5} The neutron diffraction study indicated that the phase transition of $R_2Ru_2O_7$ could be explained as one to the almost antiferromagnetically long-range ordered state, even though the low temperature phase is a spin-glass state in the macroscopic sense.⁶

In this study, we have performed magnetic susceptibility measurements on the heavy rare earth ruthenate pyrochlores $R_2Ru_2O_7$ ($R = Gd, Tb, Dy, Ho, Er, Tm, \text{ and } Yb$) in the temperature range between 1.8 K and 300 K to elucidate their magnetic behavior at lower temperatures. In addition, the specific heat for each of these compounds was measured in the temperature range between 1.8 K and 300 K.

Experimental

Sample preparation

Polycrystalline samples of ruthenium pyrochlore were prepared by decomposing well-mixed solid nitrates. The rare

earth oxides R_2O_3 ($R = Gd, Dy, Ho, Er, Tm, \text{ and } Yb$), Tb_4O_7 and ruthenium dioxide RuO_2 (all with purity >99.9%) were weighed in the correct metal ratios and dissolved in concentrated nitric acid. The excess nitric acid was removed by gentle heating. The remaining powders were slowly heated to 673 K for 3 h and heated at 1123 K for 12 h. After cooling to room temperature, the samples were crushed into powders, reground, pressed into pellets, and then reheated at 1373–1423 K, with several intermediate regrindings. $Lu_2Sn_2O_7$, which was used as the standard sample for the specific heat measurements, as will be described later was prepared from a stoichiometric mixture of Lu_2O_3 and SnO_2 (the purity of these materials is better than 99.9%). The mixture was heated at 1673 K with several intermediate regrindings.

Analysis

X-Ray powder diffraction measurements were performed with $CuK\alpha$ radiation on a Rigaku MultiFlex diffractometer equipped with a curved graphite monochromator and showed that the desired pyrochlore-type compounds $R_2Ru_2O_7$ ($R = Gd, Tb, Dy, Ho, Er, Tm, \text{ and } Yb$) and $Lu_2Sn_2O_7$ could each be prepared as a single phase. Intensity data were collected by step scanning in the range between 10° and 120° at intervals of 0.02° .

Magnetic measurements

Magnetic susceptibility measurements were performed with a SQUID magnetometer (Quantum Design MPMS model). The temperature dependence of the magnetic susceptibilities was investigated under zero-field-cooled (ZFC) and field-cooled conditions (FC). The former was measured on heating the sample to 300 K after zero-field cooling to 1.8 K. The applied magnetic field was 0.1 T. The latter was measured on cooling the sample from 300 to 1.8 K at 0.1 T. Magnetization was measured at 1.8, 5.0 and 10 K by changing the applied magnetic field between 0 T and 9 T with a commercial magnetometer (Quantum Design, PPMS model).

Specific heat measurements

The specific heat of the samples was measured in the temperature range 1.8–300 K using the relaxation technique supplied by a commercial heat capacity measurement system (Quantum Design, PPMS model). The sample in the form of a

Table 1 Curie constants C , Weiss constants θ , temperature-independent paramagnetic susceptibilities α , and effective magnetic moment of Ru^{4+} μ_{Ru} for $\text{R}_2\text{Ru}_2\text{O}_7$

	$C/\text{emu K mol}^{-1}$	θ/K	$\alpha/\text{emu K mol}^{-1}$	$\mu_{\text{Ru}}/\mu_{\text{B}}$
Gd	16.49	-10.9	—	2.58
Tb	25.12	-14.6	—	2.88
Dy	25.73	0.170	6.4×10^{-3}	3.30
Ho	25.61	0.878	6.0×10^{-3}	4.32
Er	23.02	-20.4	1.1×10^{-3}	2.20
Tm	15.77	-50.3	6.3×10^{-4}	2.41

pellet (~ 10 mg) was mounted on an aluminium plate with apiezon for better thermal contact.

Results and discussion

1. Magnetic susceptibilities

The temperature dependences of the magnetic susceptibility χ_{mol} for $\text{R}_2\text{Ru}_2\text{O}_7$ are shown in Figs. 1(a)–7(a). For all the compounds except $\text{Tb}_2\text{Ru}_2\text{O}_7$, no difference between the ZFC susceptibilities and the FC susceptibilities is observed in the range 1.8–300 K. Each reciprocal magnetic susceptibility χ_{mol}^{-1} vs. temperature is fitted by the Curie–Weiss law equation with a temperature-independent paramagnetic susceptibility, $\chi = C/(T - \theta) + \alpha$, in the paramagnetic region. The obtained Curie constants C , Weiss constants θ , and temperature-independent

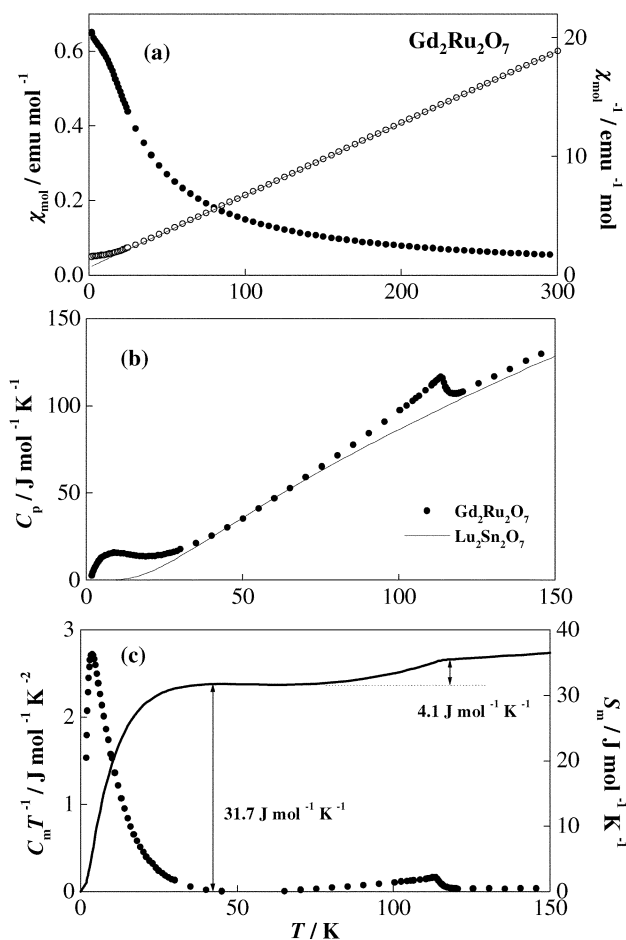


Fig. 1 (a) Temperature dependence of the magnetic susceptibility (\bullet) and the reciprocal magnetic susceptibility (\circ) for $\text{Gd}_2\text{Ru}_2\text{O}_7$. The solid line represents the Curie–Weiss fit. (b) Temperature dependence of the specific heat for $\text{Gd}_2\text{Ru}_2\text{O}_7$. The solid line represents the specific heat for $\text{Lu}_2\text{Sn}_2\text{O}_7$. (c) Temperature dependence of the magnetic specific heat divided by temperature (C_{m}/T) for $\text{Gd}_2\text{Ru}_2\text{O}_7$. The solid line represents the magnetic entropy change.

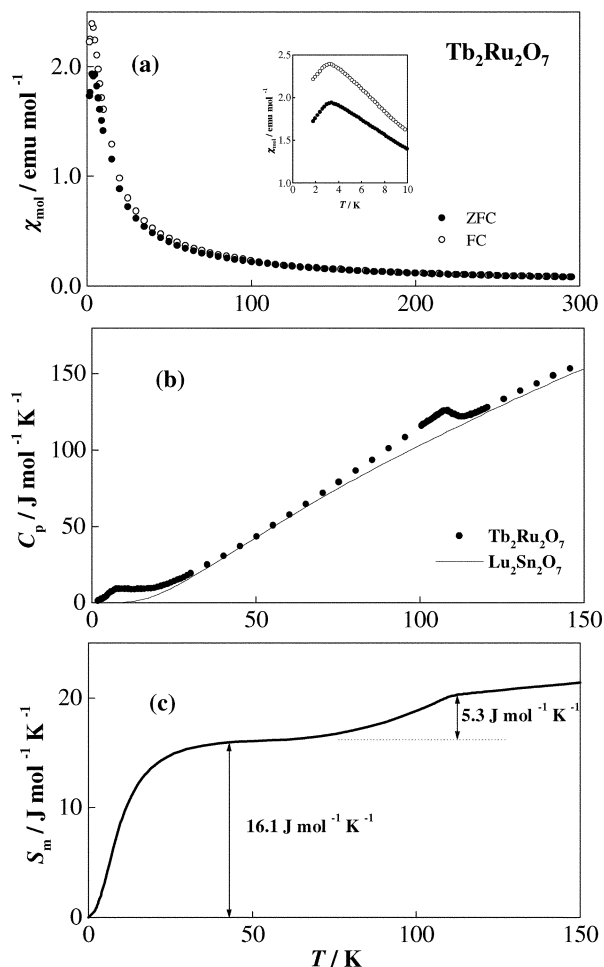


Fig. 2 (a) Temperature dependence of the susceptibilities for $\text{Tb}_2\text{Ru}_2\text{O}_7$. Filled symbols (\bullet) correspond to ZFC susceptibilities and open symbols (\circ) correspond to FC susceptibilities. The inset shows the temperature dependence of the magnetic susceptibilities below 10 K. (b) Temperature dependence of the specific heat for $\text{Tb}_2\text{Ru}_2\text{O}_7$. (c) Magnetic entropy for $\text{Tb}_2\text{Ru}_2\text{O}_7$.

paramagnetic susceptibilities α are listed in Table 1. Since a large deviation from the Curie–Weiss law is clearly seen in the susceptibilities for $\text{Yb}_2\text{Ru}_2\text{O}_7$ (Fig. 7(a)), the fitting was not carried out. This deviation may originate from the crystal field effect. These Curie constants consist of contributions from the rare earth ions and the Ru ions, *i.e.*, $C = 2(C_{\text{R}} + C_{\text{Ru}})$. The Curie constants for the rare earth ions C_{R} in these $\text{R}_2\text{Ru}_2\text{O}_7$ compounds are estimated from the isostructural $\text{R}_2\text{Ti}_2\text{O}_7$, where Ti ions are diamagnetic.^{7–9} After subtracting C_{R} from the Curie constant of $\text{R}_2\text{Ru}_2\text{O}_7$ C , the Curie constants of the Ru ions C_{Ru} were estimated and they were converted into the effective magnetic moments, μ_{Ru} , which are listed in Table 1. They are comparable to a spin-only value of $2.83 \mu_{\text{B}}$ for an $S = 1$ system, although the value for $\text{R} = \text{Ho}$ is somewhat larger. This result indicates that the Ru^{4+} ions are in the low spin state in $\text{R}_2\text{Ru}_2\text{O}_7$. The negative Weiss constants θ for $\text{R} = \text{Gd}$, Tb , Er , and Tm indicate that the predominant magnetic exchange interaction is antiferromagnetic and the positive ones for $\text{R} = \text{Dy}$ and Ho indicate the interaction is ferromagnetic. The small temperature-independent susceptibility α is considered to be a contribution of Van Vleck paramagnetism.¹⁰

No long-range magnetic ordering is observed in the magnetic susceptibility data down to 1.8 K for $\text{R} = \text{Gd}$, Dy , Ho , and Tm , while deviation from the Curie–Weiss law is observed for $\text{R} = \text{Gd}$ and Tm . The deviation below 35 K for $\text{Gd}_2\text{Ru}_2\text{O}_7$ which is shown in Fig. 1(a) can be understood as due to a splitting of the Gd magnetic levels, which will be discussed

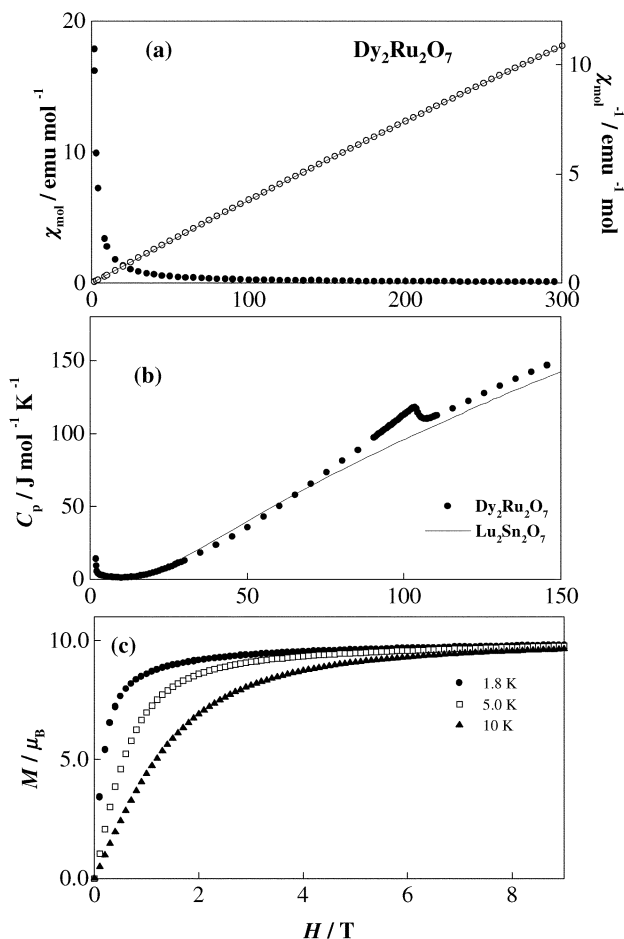


Fig. 3 (a) Temperature dependence of the magnetic susceptibility (●) and the reciprocal magnetic susceptibility (○) for $\text{Dy}_2\text{Ru}_2\text{O}_7$. The solid line represents the Curie–Weiss fit $\chi = C/(T - \theta) + \alpha$. (b) Temperature dependence of the specific heat for $\text{Dy}_2\text{Ru}_2\text{O}_7$. (c) Magnetization per formula unit vs. magnetic field for $\text{Dy}_2\text{Ru}_2\text{O}_7$ at 1.8, 5.0, and 10 K.

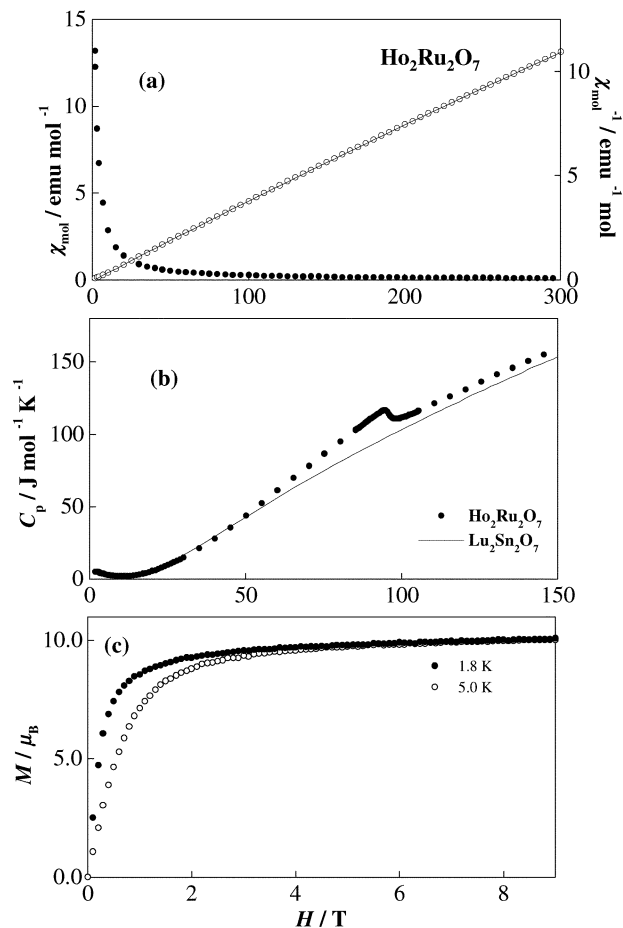


Fig. 4 (a) Temperature dependence of the magnetic susceptibility (○) and the reciprocal magnetic susceptibility (○) for $\text{Ho}_2\text{Ru}_2\text{O}_7$. The solid line represents the Curie–Weiss fit $\chi = C/(T - \theta) + \alpha$. (b) Temperature dependence of the specific heat for $\text{Ho}_2\text{Ru}_2\text{O}_7$. (c) Magnetization per formula unit vs. magnetic field for $\text{Ho}_2\text{Ru}_2\text{O}_7$ at 1.8 and 5.0 K.

later. In $\text{Tm}_2\text{Ru}_2\text{O}_7$, the Tm^{3+} ions occupy the $\bar{3}m$ environment with nearly cubic symmetry. Since the ground state of the Tm^{3+} ion is a singlet in the presence of a cubic crystal field,¹¹ the magnetic susceptibility of the Tm^{3+} ion should exhibit temperature-independent behavior at lower temperatures. It is considered that an almost temperature-independent susceptibility found in the temperature region between 10 and 70 K (Fig. 6(a)) corresponds to this theoretical notion.

With further decreasing temperature, the temperature dependence of the magnetic susceptibility χ_{mol} for $\text{R} = \text{Tb}$, Er , and Yb shows an antiferromagnetic transition at 3.4, 5.4, and 6.3 K, respectively (see Figs. 2, 5 and 7(a)). These magnetic anomalies are considered to be associated with the magnetic interactions between the rare earth ions, because the magnetic ordering of Ru^{4+} ions in these compounds occurs at 83–110 K, as will be described later.

2. Specific heats

The specific heats C_p for $\text{R}_2\text{Ru}_2\text{O}_7$ as a function of temperature are shown in Figs. 1(b)–7(b). They show a λ -type specific heat anomaly for all the compounds and this is in agreement with the results of other workers.⁵ The temperatures at which the λ -type specific heat anomalies were observed are listed in Table 2 and they become lower with decreasing ionic radius of the rare earth in these ruthenium pyrochlores. These λ -type anomalies can be considered to be associated with the long-range magnetic ordering of Ru^{4+} ions, because similar anomalies were observed for $\text{Y}_2\text{Ru}_2\text{O}_7$ and $\text{Lu}_2\text{Ru}_2\text{O}_7$ in which Ru^{4+} ions are the only magnetic ions.^{3,4} At a first glance, no

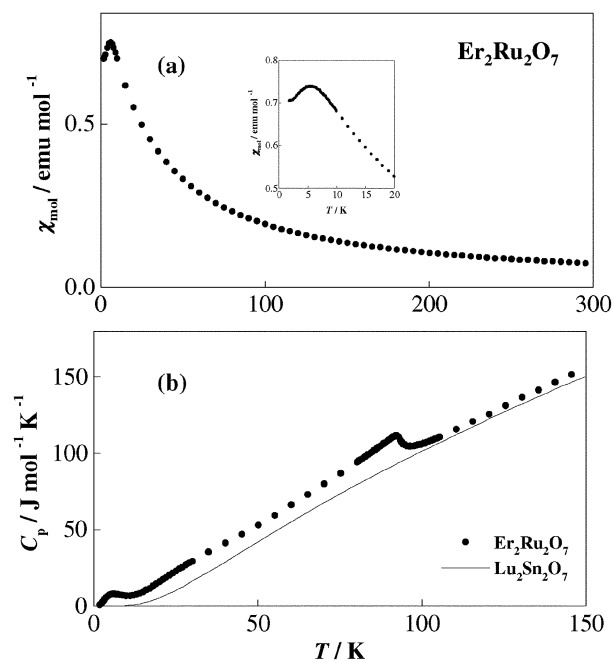


Fig. 5 (a) Temperature dependence of the susceptibilities for $\text{Er}_2\text{Ru}_2\text{O}_7$. The inset shows the temperature dependence of the magnetic susceptibilities below 20 K. (b) Temperature dependence of the specific heat for $\text{Er}_2\text{Ru}_2\text{O}_7$.

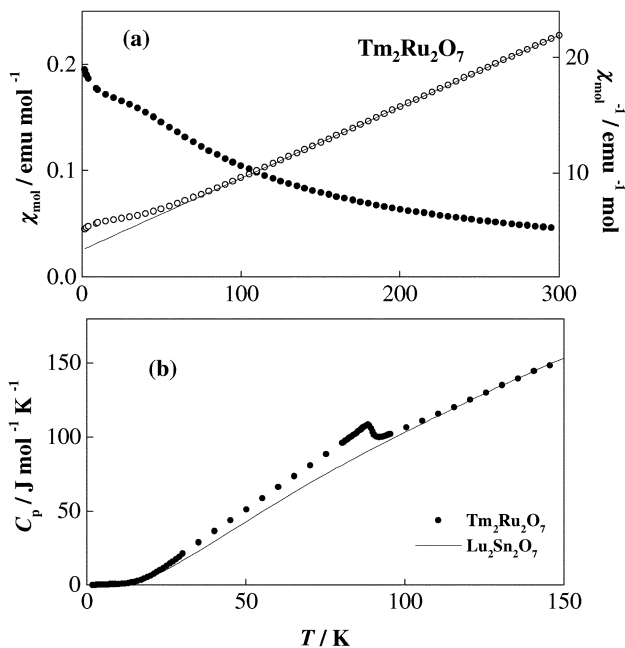


Fig. 6 (a) Temperature dependence of the magnetic susceptibility (●) and the reciprocal magnetic susceptibility (○) for $\text{Tm}_2\text{Ru}_2\text{O}_7$. The solid line represents the Curie–Weiss fit $\chi = C/(T - \Theta) + \alpha$. (b) Temperature dependence of the specific heat for $\text{Tm}_2\text{Ru}_2\text{O}_7$.

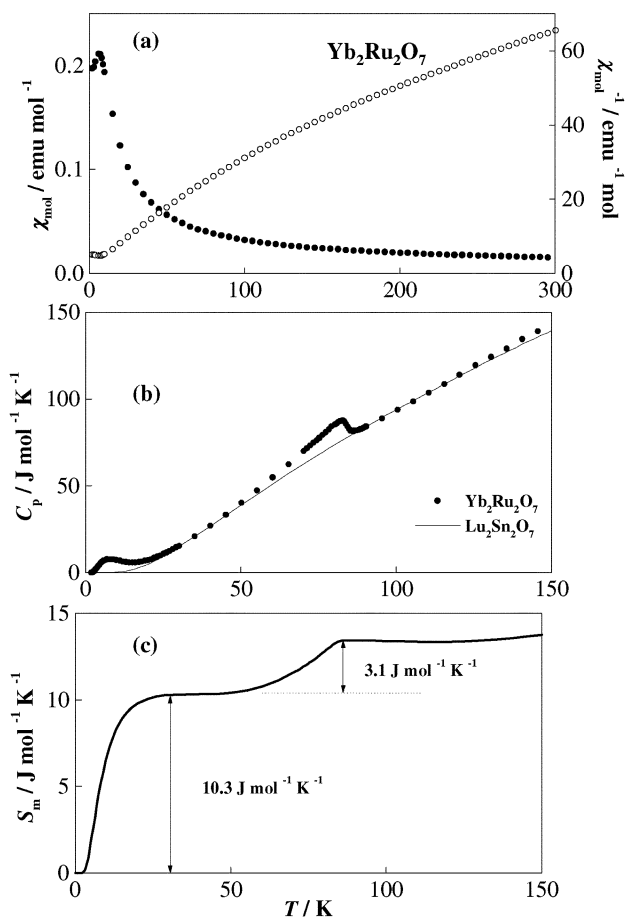


Fig. 7 (a) Temperature dependence of the magnetic susceptibility (●) and the reciprocal magnetic susceptibility (○) for $\text{Yb}_2\text{Ru}_2\text{O}_7$. (b) Temperature dependence of the specific heat for $\text{Yb}_2\text{Ru}_2\text{O}_7$. (c) Magnetic entropy for $\text{Yb}_2\text{Ru}_2\text{O}_7$.

obvious magnetic anomaly is seen in the magnetic susceptibility vs. temperature curve at the temperature which the λ -type specific heat anomaly was observed, while a small change of

Table 2 Temperatures of anomalies found in specific heat and susceptibility measurements for $\text{R}_2\text{Ru}_2\text{O}_7$

	λ -Type anomaly in specific heat/K	Magnetic entropy change at λ -type anomaly/ $\text{J mol}^{-1} \text{K}^{-1}$	Magnetic anomaly in susceptibility/K
Gd	113	4.1	—
Tb	110	5.3	3.4
Dy	103	3.5	—
Ho	94	6.4	—
Er	92	—	5.4
Tm	88	—	—
Yb	83	3.1	6.3

the slope is detected at the corresponding temperature in the χT vs. temperature curve. This is probably due to the fact that the large magnetic moment of the rare earth ions makes the magnetic ordering of Ru^{4+} ions invisible in the magnetic susceptibility vs. temperature curve for $\text{R}_2\text{Ru}_2\text{O}_7$. For $\text{R} = \text{Tb}$, a slight difference between the ZFC and FC susceptibilities is observed below ca. 110 K (Fig. 2(a)). At the same temperature, a λ -type specific heat anomaly was observed (Fig. 2(b)). It may be inferred from this result that the magnetic state of heavy rare earth ruthenate pyrochlores also transforms to a spin-glass state below the transition temperatures, which is the same as the case for $\text{R}_2\text{Ru}_2\text{O}_7$ ($\text{R} = \text{Pr}–\text{Eu}$).⁴

With further decreasing temperature, specific heat anomalies are observed for all compounds except $\text{Tm}_2\text{Ru}_2\text{O}_7$. There is a broad Schottky-like anomaly in the specific heat data below 35 K for $\text{R} = \text{Gd}_2\text{Ru}_2\text{O}_7$ (Fig. 1(b)), which corresponds to the deviation from the Curie–Weiss law in the susceptibility data shown in Fig. 1(a). As shown in Figs. 3(b) and 4(b), the specific heat for the $\text{R} = \text{Dy}$ and Ho compounds increases with decreasing temperature below 10 and 20 K, respectively. Unfortunately, the peak for the specific heat anomaly is not detected in these experiments ($T \geq 1.8$ K). It may be inferred from the positive Θ and the increase of the specific heat at lower temperatures that there is a ferromagnetic transition below 1.8 K for both these compounds. The field dependence of the magnetization at 1.8, 5.0, and 10 K is shown in Figs. 3(c) and 4(c). No magnetic hysteresis loop was observed at any temperature. These magnetization vs. the applied field curves could not be described by the free ion Brillouin function for Dy^{3+} ($J = 15/2$) and Ho^{3+} ($J = 8$), but rather, were observed to saturate at approximately half the theoretical value $2g_J J = 20$. This behavior may originate from strong single-ion anisotropy for Dy^{3+} and Ho^{3+} . For isostructural $\text{Dy}_2\text{Ti}_2\text{O}_7$ and $\text{Ho}_2\text{Ti}_2\text{O}_7$, it has been reported that there is only one direction of easy magnetization.^{12–14}

For the $\text{R} = \text{Tb}$, Er , and Yb compounds, another broad anomaly is observed in their specific heat vs. temperature curves at 9, 6, and 7 K, respectively. These broad specific heat anomalies correspond to the antiferromagnetic transitions found in the magnetic susceptibility vs. temperature curves. The absence of the λ -type specific heat anomaly indicates that the magnetic transition observed in the susceptibility vs. temperature curves is due to short-range magnetic ordering.

3. Magnetic entropy

Next, we will estimate the magnetic entropy change associated with the magnetic transitions from the specific heat data. To calculate the magnetic contribution to the specific heat, we have to subtract the electronic and lattice contributions from the total specific heat. In order to estimate them, we prepared a nonmagnetic compound $\text{Lu}_2\text{Sn}_2\text{O}_7$ (which is isomorphous with $\text{R}_2\text{Ru}_2\text{O}_7$). In Figs. 1(b)–7(b), the specific heat data for $\text{Lu}_2\text{Sn}_2\text{O}_7$ are also shown. If we assume that the electronic and lattice contributions to the specific heat are equal between $\text{R}_2\text{Ru}_2\text{O}_7$ and $\text{Lu}_2\text{Sn}_2\text{O}_7$, the magnetic specific heat (C_m) for

$R_2Ru_2O_7$ is obtained by subtracting the specific heat of $Lu_2Sn_2O_7$. Fig. 1(c) shows the magnetic specific heat of $Gd_2Ru_2O_7$ divided by temperature (C_m/T) and the magnetic entropy change (S_m) as a function of temperature. The magnetic specific heat below 1.8 K was estimated by extrapolating the higher temperature data to lower temperatures. The magnetic entropy change associated with the magnetic transition is calculated by integrating.

$$S_m(T) = \int_0^T (C_m/T) dT \quad (1)$$

Since a broad Schottky-like anomaly is smeared out over a large temperature range, the entropy changes for the $R = Er$ and Tm compounds cannot be determined. For the other compounds, the magnetic entropy changes associated with the magnetic ordering for Ru^{4+} ions at 83–113 K are estimated to be 3.1–6.4 $J mol^{-1} K^{-1}$ and they are listed in Table 2. These values are much lower than the expected $2R \ln(2S + 1) = 2R \ln 3 = 18.3 J mol^{-1} K^{-1}$, where R is the molar gas constant, if the Ru^{4+} ions are in the low spin state ($S = 1$) in $R_2Ru_2O_7$. We attempted to calculate the magnetic entropy for $Lu_2Ru_2O_7$ in which Ru^{4+} ions are the only magnetic ions.⁴ The derived magnetic entropy for the λ -type anomaly is 3.6 $J mol^{-1} K^{-1}$. This value is comparable to those for the other $R_2Ru_2O_7$ and also much lower than $2R \ln 3$. A similar result that magnetic entropy values corresponding to spin-glass-like ordering reach only about 14–31% of the expected ones was reported for the isostructural $R_2Mo_2O_7$.¹⁵ The reduction of the magnetic entropy may possibly be a common trend for rare earth pyrochlores having the 4d electrons.

Fig. 1(c) shows that the magnetic entropy change of the lower temperature Schottky-like anomaly for $R = Gd$ is found to be 31.7 $J mol^{-1} K^{-1}$, which is close to the value $2R \ln 8 = 34.6 J mol^{-1} K^{-1}$ assuming free ion behavior for the Gd^{3+} (the $^8S_{7/2}$ state). This result indicates that the ground state of the Gd^{3+} ion in $Gd_2Ru_2O_7$ has eight-fold degeneracy. The specific heat anomaly below 35 K can be understood as due to a splitting of the Gd magnetic levels induced by an internal magnetic field, which is caused by the ordering of the Ru^{4+} ions, like the specific heat anomaly for an isostructural gadolinium molybdate pyrochlore $Gd_2Mo_2O_7$.¹⁵ The specific heat behavior in the low temperature region for $Gd_2Ru_2O_7$ is similar to that for $Gd_2Mo_2O_7$. Fig. 2(c) shows that the magnetic entropy change corresponds to the anomaly at 3.4 K for $Tb_2Ru_2O_7$ and it is found to be 16.1 $J mol^{-1} K^{-1}$, which is larger than the expected value $2R \ln 2 = 11.5 J mol^{-1} K^{-1}$ for a doublet ground state of Tb^{3+} . This discrepancy may arise from an inappropriate estimation for the magnetic entropy below 1.8 K. The magnetic entropy change for $Yb_2Ru_2O_7$ is shown in Fig. 7(c). The magnetic entropy change due to the antiferromagnetic transition at 7 K is found to be 10.3 $J mol^{-1} K^{-1}$ which is close to the value $2R \ln 2 = 11.5 J mol^{-1} K^{-1}$. The Yb^{3+} ion has the configuration $4f^{13}$ which gives rise to a $^2F_{7/2}$ ground multiplet and the eight-fold ground-state degeneracy for $^2F_{7/2}$ will be split into a pair of doublets and a quartet in a cubic crystal field.¹¹ This result of the magnetic entropy change

indicates that the degeneracy of the ground state for Yb^{3+} should be a doublet.

Conclusions

In this study, we focus our attention on the magnetic properties of heavy rare earth ruthenate pyrochlores $R_2Ru_2O_7$, where $R = Gd$ – Yb . For all of the compounds, a λ -type anomaly is clearly observed at 83–113 K in the specific heat vs. temperature curve indicating the long-range ordering of Ru^{4+} ions, although such an anomaly is not visible in the magnetic susceptibility vs. temperature curve. For $R = Tb$, Er , and Yb , magnetic anomalies are observed at 3.4, 5.4, and 6.3 K, respectively, in the magnetic susceptibility vs. temperature curve. These magnetic anomalies are considered to be associated with the magnetic interactions between the rare earth ions. The specific heat measurements reveal that Gd^{3+} and Yb^{3+} ions in $Gd_2Ru_2O_7$ and $Yb_2Ru_2O_7$ have eight-fold and two-fold degenerate ground states, respectively. The broad specific heat anomaly indicates the presence of short-range magnetic interactions between the rare earth ions for $R = Tb$, Er , and Yb . In pyrochlore compounds, rare earth atoms (and also ruthenium atoms) form a three-dimensional network of corner-sharing tetrahedra. Such an arrangement leads to a very high degree of magnetic frustration if the nearest-neighbor interactions are antiferromagnetic. It is considered that the magnetic anomalies found for $R_2Ru_2O_7$ are caused by a geometrical peculiarity of the pyrochlore structure.

References

- 1 N. Taira, M. Wakeshima and Y. Hinatsu, *J. Solid State Chem.*, 1999, **144**, 216.
- 2 N. Taira, M. Wakeshima and Y. Hinatsu, *J. Phys.: Condens. Matter.*, 1999, **11**, 6983.
- 3 S. Yoshii and M. Sato, *J. Phys. Soc. Jpn.*, 1999, **68**, 3034.
- 4 N. Taira, M. Wakeshima and Y. Hinatsu, *J. Solid State Chem.*, 2000, **152**, 441.
- 5 M. Ito, Y. Yasui, M. Kanada, H. Harashina, S. Yoshii, K. Murata, M. Sato, H. Okumura and K. Kakurai, *J. Phys. Chem. Solids*, 2001, **62**, 337.
- 6 S. Yoshii and M. Sato, *J. Phys. Soc. Jpn.*, 2000, **69**, 888.
- 7 N. P. Raju, M. Dion, M. J. P. Gingras, T. E. Mason and J. E. Greedan, *Phys. Rev. B*, 1999, **59**, 14489.
- 8 M. J. P. Gingras, B. C. den Hertog, M. Faucher, J. S. Gardner, S. R. Dunsiger, L. J. Chang, B. D. Gaulin, N. P. Raju and J. E. Greedan, *Phys. Rev. B*, 2000, **62**, 6496.
- 9 S. T. Bramwell, M. N. Field, M. J. Harris and I. P. Parkin, *J. Phys.: Condens. Matter.*, 2000, **12**, 483.
- 10 J. H. Van Vleck, *Theory of Electric and Magnetic Susceptibilities*, Clarendon, Oxford, 1932.
- 11 K. R. Lea, M. J. M. Leask and W. P. Wolf, *J. Phys. Chem. Solids*, 1962, **23**, 1381.
- 12 D. J. Flood, *J. Appl. Phys.*, 1974, **45**, 4041.
- 13 H. Fukazawa, R. G. Melko, R. Higashinaka, Y. Maeno and M. J. P. Gingras, *Phys. Rev. B*, 2002, **65**, 054410.
- 14 A. L. Cornelius and J. S. Gardner, *Phys. Rev. B*, 2001, **64**, 060406.
- 15 N. P. Raju, E. Gmelin and R. K. Kremer, *Phys. Rev. B*, 1992, **46**, 5405.